



**UNIVERSITY OF LEEDS**

This is a repository copy of *A new model of ozone stress in wheat including grain yield loss and plant acclimation to the pollutant*.

White Rose Research Online URL for this paper:  
<https://eprints.whiterose.ac.uk/162631/>

Version: Accepted Version

---

**Article:**

Droutsas, I [orcid.org/0000-0002-5123-3379](https://orcid.org/0000-0002-5123-3379), Challinor, AJ [orcid.org/0000-0002-8551-6617](https://orcid.org/0000-0002-8551-6617), Arnold, SR [orcid.org/0000-0002-4881-5685](https://orcid.org/0000-0002-4881-5685) et al. (2 more authors) (2020) A new model of ozone stress in wheat including grain yield loss and plant acclimation to the pollutant. *European Journal of Agronomy*, 120. 126125. ISSN 1161-0301

<https://doi.org/10.1016/j.eja.2020.126125>

---

© 2020 Published by Elsevier B.V. This manuscript version is made available under the CC-BY-NC-ND 4.0 license <http://creativecommons.org/licenses/by-nc-nd/4.0/>

**Reuse**

This article is distributed under the terms of the Creative Commons Attribution-NonCommercial-NoDerivs (CC BY-NC-ND) licence. This licence only allows you to download this work and share it with others as long as you credit the authors, but you can't change the article in any way or use it commercially. More information and the full terms of the licence here: <https://creativecommons.org/licenses/>

**Takedown**

If you consider content in White Rose Research Online to be in breach of UK law, please notify us by emailing [eprints@whiterose.ac.uk](mailto:eprints@whiterose.ac.uk) including the URL of the record and the reason for the withdrawal request.



[eprints@whiterose.ac.uk](mailto:eprints@whiterose.ac.uk)  
<https://eprints.whiterose.ac.uk/>

# A new model of ozone stress in wheat including grain yield loss and plant acclimation to the pollutant

I. Droutsas<sup>a,b,\*</sup>, A. J. Challinor<sup>a,b</sup>, S. R. Arnold<sup>a,b</sup>, T. N. Mikkelsen<sup>c</sup>, E. M. Ø. Hansen<sup>d</sup>

<sup>a</sup>*Institute for Climate and Atmospheric Science, School of Earth and Environment, University of Leeds, LS2 9JT Leeds, UK*

<sup>b</sup>*Priestley International Centre for Climate, University of Leeds, LS2 9JT, Leeds, UK*

<sup>c</sup>*Department of Environmental Engineering, Technical University of Denmark, DK-2800 Lyngby, Denmark*

<sup>d</sup>*Department of People and Technology, Roskilde University, Universitetsvej 1, DK-4000 Roskilde, Denmark*

---

## Abstract

Surface ozone ( $O_3$ ) is an important air pollutant globally and enhanced concentrations lead to crop yield penalties in many parts of the world. Crop models simulate production and yield and they are often used for various applications. However, most of the existing models neglect the effect of  $O_3$  and only limited parameterization schemes exist. In addition, the existing  $O_3$  modelling approaches do not take into account the plant acclimation to the pollutant as a mechanism of survival and maintenance of performance. Here, we introduce a simple modelling method to simulate the  $O_3$  damage to wheat with consideration of the plant acclimation process. The  $O_3$  parameterization scheme was incorporated into the GLAM-Parti crop model, resulting in a new model version GLAM-ROC (i.e. GLAM - Relative Ozone Concentrations). The new model simulates the effect of  $O_3$  on crop growth and development and was evaluated against data from control-environment chambers with high  $O_3$  concentration levels and variable duration of exposure to the pollutant. GLAM-ROC successfully reproduced the observed plant response to  $O_3$  as well as the final biomass and yield. The incorporation of plant acclimation allowed the prediction of crop yield loss at variable duration of  $O_3$  exposure. The statistical response formula neglected the acclimation process and overestimated the relative  $O_3$  damage to yield by 56.5%, when fumigation increased from 32 to 106 days. We conclude that the plant acclimation to chronic  $O_3$  environment is significant and should be taken into account for the effect of  $O_3$  on wheat performance and yield.

**Keywords:** Crop model, Ozone, Wheat, Acclimation, GLAM-ROC, GLAM-PARTI

---

## 1. Introduction

Ground-level ozone ( $O_3$ ) is a highly phytotoxic air pollutant at global scale (Ashmore, 2005; Ainsworth, 2017). Current  $O_3$  levels induce crop yield damage and lead to decreased food supply and economic loss

---

\*Corresponding author

Email address: eegdr@leeds.ac.uk (I. Droutsas)

(Emberson et al., 2009; McGrath et al., 2015). Avnery et al. (2011) estimated that global yields of soybean and wheat were reduced by up to 14 and 15% respectively for the year 2000 due to O<sub>3</sub> pollution. Mills et al. (2018) estimated that in highly polluted regions of N India and NW China the O<sub>3</sub> damage to wheat yield exceeded 15% on average for the years 2010 - 2012. O<sub>3</sub> concentrations are projected to remain enhanced in many regions in the future, potentially posing serious threat to agriculture (Sicard et al., 2017).

The main mechanisms through which O<sub>3</sub> affects crops are by inhibiting photosynthesis, accelerating the plant senescence rate and causing leaf chlorosis or necrosis under acute exposure (Heath, 1994; Farage and Long, 1999; Fiscus et al., 2005). These effects result in decreased photosynthate allocation to the grain, reduced productivity and lower yield (Wilkinson et al., 2012). The range of effects depends upon the concentration level of the pollutant, the time and duration of exposure (Heath et al., 2009), the plant sensitivity (Van Goethem et al., 2013) and the stage of plant development (Tiedemann and Pfähler, 1994; Mulholland et al., 1998).

The effect of O<sub>3</sub> on crop yield has been extensively studied and various modelling approaches have been suggested. Initially, different metrics were developed to link the plant O<sub>3</sub> exposure to the reduction in grain yield. These metrics accumulate the O<sub>3</sub> concentration during the crop-growing season (e.g. AOT40, M7, SUM06, W126) and relate the effect to yield according to a statistical response function (e.g. Fuhrer et al., 1997; Mauzerall and Wang, 2001). However, various interactions between the crops and their surrounding environment modify the magnitude of this relationship (Musselman et al., 2006). This is a major limitation of exposure-based approaches and so O<sub>3</sub> effects were later introduced into more complex models of plant growth and development.

The family of more complex models tend to use stomatal flux parameterizations (e.g. Emberson et al., 2000; Pleijel et al., 2007) such as those found in crop models (e.g. Ewert and Porter, 2000; Schauburger et al., 2019). These models can improve upon the exposure-based estimation of O<sub>3</sub> damage to crop productivity and yield by simulating the stomatal limitations which regulate O<sub>3</sub> uptake by the plants (Challinor et al., 2009; Pleijel et al., 2004). Nevertheless, the modelling of stomatal conductance is difficult and it is not clear which of the many models of different complexity (Damour et al., 2010) is closest to reality. Modelled responses to CO<sub>2</sub> concentration, temperature, air humidity, light and soil water content differ (Buckley and Mott, 2013), resulting in different errors in the calculation of O<sub>3</sub> uptake and damage.

Plants can adjust their physiological and metabolic processes to enhance their stress tolerance over time (Bruce et al., 2007). Under long-term O<sub>3</sub> exposure, the plant anti-oxidative enzyme activity increases (Gille-

spie et al., 2011, 2012), working as a mechanism of defence in favour of closing stomata to avoid take-up of O<sub>3</sub> (Feng et al., 2016). This acclimation mechanism allows stomata to remain partially open and support gas exchange for photosynthesis, thus avoiding high reductions in biomass accumulation (Chen et al., 2011). The acclimation process in stress environments improves the plant response to the stressor (Kollist et al., 2018) and leads to optimisation of productivity and yield. Held et al. (1991) exposed radish plants to high O<sub>3</sub> either six days after germination or three days later and found that the plants which were exposed to the the pollutant for the longer period exhibited higher dry mass than the plants exposed to O<sub>3</sub> later, implying an acclimation mechanism. Trees can also compensate for the negative O<sub>3</sub> effects by activating acclimation mechanisms. Mikkelsen and Ro-Poulsen (1994) reported higher photosynthesis levels of Norway spruce in the morning before 8-h daily O<sub>3</sub> fumigation, as well as five days post-O<sub>3</sub> fumigation in comparison with non-fumigated trees. Crop models do not usually parameterize for plant acclimation to chronic O<sub>3</sub> stress. One barrier to the development of acclimation parameterizations in crop models is that the models are not evaluated under variable duration of exposure to O<sub>3</sub>.

The purpose of this study is to incorporate the effect of O<sub>3</sub> into a crop model by accounting for the concentration level of the pollutant, the stage of plant development and the duration of plant exposure. The wheat crop was selected as case study since it is particularly sensitive to O<sub>3</sub> (Barnes et al., 1990; Farage et al., 1991; Burney and Ramanathan, 2014), an important staple crop at global level (FAO et al., 2017) and there is excellent data availability. The GLAM-Parti crop model was used to incorporate the effect of O<sub>3</sub> on wheat, resulting in a new model version called GLAM-ROC (i.e. GLAM-Relative Ozone Concentrations). Prior to the incorporation of the O<sub>3</sub> effect, the allometric relationships for partitioning plant biomass in GLAM-Parti were extended to the full crop cycle, since the model was previously developed with the GLAM approach for post-anthesis crop growth and development.

## **2. Materials and Methods**

### *2.1. Wheat varieties and growing conditions*

Two modern spring wheat varieties were considered in this study, Lennox (Saaten-Union) used in southern France and KWS Bittern (DanishAgro) used in Denmark. Lennox was used for the development of the O<sub>3</sub> algorithm in the model and KWS Bittern for the model evaluation. The plants were grown in 24 m<sup>2</sup> chambers in the RERAF (Risoe Environmental Risk Assessment Facility) climate phytotron at the Technical University of Denmark, Campus Risø, Roskilde. The plants were sown in 11 L pots filled with 4 kg of sphagnum (Pindstrup

Substrate No. 4, Pindstrup Mosebrug A/S, Ryomgaard, Denmark) and reduced to eight plants after germination, corresponding to  $\sim 165$  plants  $m^{-2}$ . Light intensity in the chambers was approximately 400 mol photons  $m^{-2} s^{-1}$  PAR (photosynthetically active radiation) at canopy height and was provided for 16 h  $d^{-1}$ . The growing conditions in the chambers are shown in Table 1. The plants were watered three times a week to ensure full water supply. No additional nutrients were added to the pots since the sphagnum was nutrient enriched. Both varieties were represented by five replicates in each treatment. Detailed description of the experimental set-up is given in Hansen et al. (2019), Frenck et al. (2011) and Ingvordsen et al. (2015).

Treatment	Temperature, day/night ( $^{\circ}C$ )	Humidity, day/night (%)	[O <sub>3</sub> ] (ppb)	[CO <sub>2</sub> ] (ppm)
Control	19.4 $\pm$ 2.5 / 13.8 $\pm$ 4.1	53.7 $\pm$ 5.3 / 65.8 $\pm$ 8.3	6.4 $\pm$ 2.1	534 $\pm$ 109
Episodic	19.4 $\pm$ 2.5 / 14.0 $\pm$ 4.1	54.2 $\pm$ 5.2 / 65.5 $\pm$ 8.0	84.5 $\pm$ 28.1	539 $\pm$ 109
Chronic	19.4 $\pm$ 2.5 / 13.9 $\pm$ 4.1	53.7 $\pm$ 5.4 / 65.5 $\pm$ 8.3	78.8 $\pm$ 32.4	537 $\pm$ 111

Table 1: Mean and standard deviation of growing conditions in RERAF chambers for wheat cultivars Lennox and KWS Bittern.

## 2.2. Ozone treatments

O<sub>3</sub> was generated by UV Pro 550 A ozone generators (Crystal Air Products and Services, Langley, BC, Canada). The experiments included 3 levels of fumigation: i) no O<sub>3</sub> enrichment (Control); ii) episodic O<sub>3</sub> exposure (Episodic) ; and iii) full-time O<sub>3</sub> exposure (Chronic) (Fig. 1 and Table 1). In the Control treatment, O<sub>3</sub> concentration in the climate chambers was 6.4  $\pm$  2.1 ppb during the whole crop cycle. In the Chronic treatment, the plants were exposed to 78.8  $\pm$  32.4 ppb O<sub>3</sub> concentration during the daylight hours from sowing (Zadoks Stage 01 - ZS 01) to harvest maturity (ZS 99). In the Episodic treatment, O<sub>3</sub> concentration was 84.5  $\pm$  28.1 ppb during the daylight hours and the duration of plant exposure was from the first node stage (ZS 31) until anthesis was complete (ZS 69). During the night, in both the Chronic and Episodic treatment, O<sub>3</sub> concentration was reduced to the Control level.

## 2.3. Plant measurements and calculation of evapotranspiration and water use efficiency

At the end of the experiment, the plants were harvested and dried for 48 h at 80  $^{\circ}C$ . The above-ground biomass and grain yield were measured in  $g\ pot^{-1}$  and were converted to  $g\ m^{-2}$  using the pot dimensions. This allowed direct comparison between the observations and the model output. The plant water consumption ( $g\ pot^{-1}$ ) was calculated as the difference in pot weight between two consecutive measurements. Assuming that the increase in plant weight between two measurements was negligible, we calculated canopy evapotranspi-

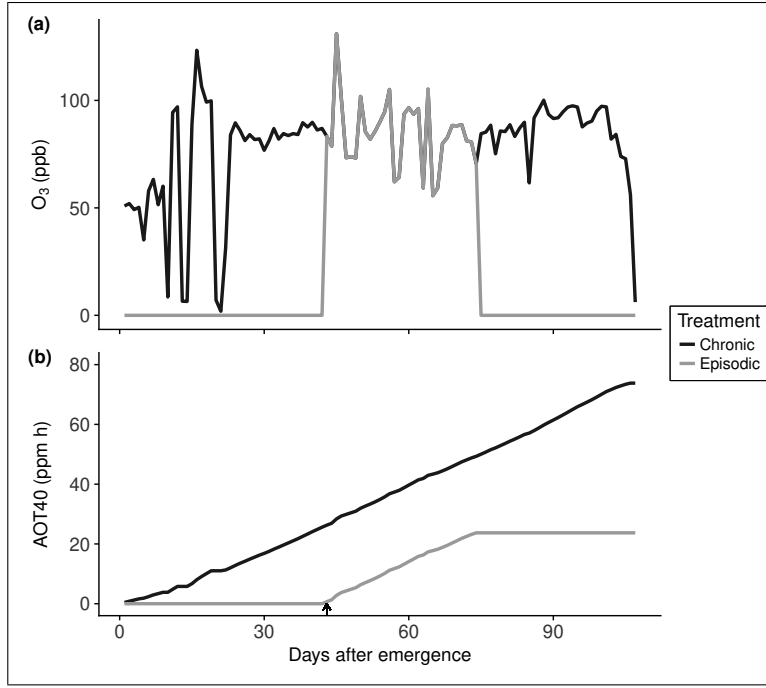


Figure 1: (a) Daily mean  $O_3$  concentration (ppb) and (b) cumulative  $O_3$  exposure above 40 ppb (AOT40) calculated from hourly  $[O_3]$  in Chronic and Episodic treatment. Arrow indicates day when plants reached ZS 31 (Zadoks stage 31).

ration (ET) (mm) as following:

$$ET = ((Wp_n - Wp_{n+1})/\rho \cdot pot) \cdot 1000mm/m \quad (1)$$

where  $Wp_n$  and  $Wp_{n+1}$  are the pot weight directly after the  $n$  irrigation (kg) and directly before the  $n+1$  irrigation (kg) respectively,  $pot$  is the number of pots per  $m^2$  and  $\rho$  is water density ( $997 \text{ kg m}^3$ ). Harvest index (HI) was calculated as the ratio of grain yield to above-ground biomass.

The biomass, grain yield, ET, HI and water use efficiency (WUE) of Lennox and KWS Bittern wheat in the experiments were calculated as the mean of the 5 replicates. The replicate 2 of Lennox in the Control and the replicate 5 of KWS Bittern in the Chronic treatment were disregarded due to errors in the measurements of pot weight. Also WUE ( $\text{g m}^{-2} \text{ mm}^{-1}$ ) was defined as the ratio of the above-ground biomass ( $\text{g m}^{-2}$ ) to total ET (mm) at harvest.

#### 2.4. Ozone metrics

The AOT40 index (Accumulated ozone exposure above a threshold of 40 ppbv) was calculated as follows:

$$AOT40 = \sum_{i=1}^n DOE40_i \quad (2)$$

where  $n$  is the number of days in the growing season,  $i$  is the day index and  $DOE40$  is the daily  $O_3$  exposure (ppm h) defined as:

$$DOE40 = \sum_{j=1}^m \max([O_3]_j - 40ppb, 0) \quad (3)$$

where  $[O_3]$  is the one hour mean  $O_3$  concentration (ppb),  $m$  is the number of daylight hours per day and  $j$  is the hour index.

### 2.5. GLAM-Parti model

The GLAM-Parti crop model was developed based on the General Large Area Model for annual crops (GLAM) which is a relatively simple model designed to operate at regional scale (Challinor et al., 2004). The model was selected for the incorporation of the effect of  $O_3$  on wheat, since it was developed with the SEMAC approach (Simultaneous Equation Modelling for Annual Crops), a novel crop modelling methodology which provides with a consistent representation of abiotic stresses and ensures internal consistency in the simulation of crop growth and development under environmental stress conditions (Droutsas et al., 2019). GLAM-Parti uses transpiration efficiency to simulate crop growth and allometric relationships for partitioning the biomass to the plant compartments. The daily potential evapotranspiration is calculated by the Priestley-Taylor approach and is partitioned into potential evaporation and potential transpiration. The actual transpiration is computed from the potential transpiration rate by taking into account the soil water content. The transpiration is multiplied by the transpiration efficiency to return the daily biomass growth.

Two major modifications were implemented into GLAM-Parti for this study. Firstly, the canopy SLA was expressed as function of LAI (see Appendix A.1). In addition, the plant biomass partitioning scheme with allometric relationships was extended to the post-anthesis period (see Appendix A.2). This method replaced the previously used GLAM approach for simulating crop growth and development after anthesis in GLAM-Parti.

### 2.6. GLAM-ROC development

GLAM-ROC is the version of GLAM-Parti which incorporates the effect of  $O_3$  on crop growth and development. The  $O_3$  damage to wheat was introduced into the model by reducing the canopy ET as well as transpiration efficiency (TE) in daily time step. The effect of  $O_3$  on ET was related to the AOT40 index and the reduction in TE was expressed as function of  $[O_3]$ . An acclimation factor was introduced to simulate the plant adjustment to stress conditions with increased  $O_3$  exposure. Harvest Index was also reduced to account for decreased allocation of assimilates to the grains under exposure to enhanced  $O_3$  during the grain-filling period.

### 2.6.1. Modelling ozone effects on evapotranspiration

Plant exposure to O<sub>3</sub> decreases leaf transpiration due to stomatal closure (Temple, 1986; Bernacchi et al., 2011), which may have widespread implications for atmospheric moisture and climate (Arnold et al., 2018; Lombardozi et al., 2012). Data analysis was conducted to examine the effect of O<sub>3</sub> on cumulative evapotranspiration (CET) during the exposure to the pollutant. CET was calculated as:

$$CET = \sum_{i=1}^n ET_i \quad (4)$$

where ET is canopy evapotranspiration, i is the day index and n is the number of days after planting. Data from the variety Lennox was used to compare the differences in CET between the Control, Chronic and Episodic treatment.

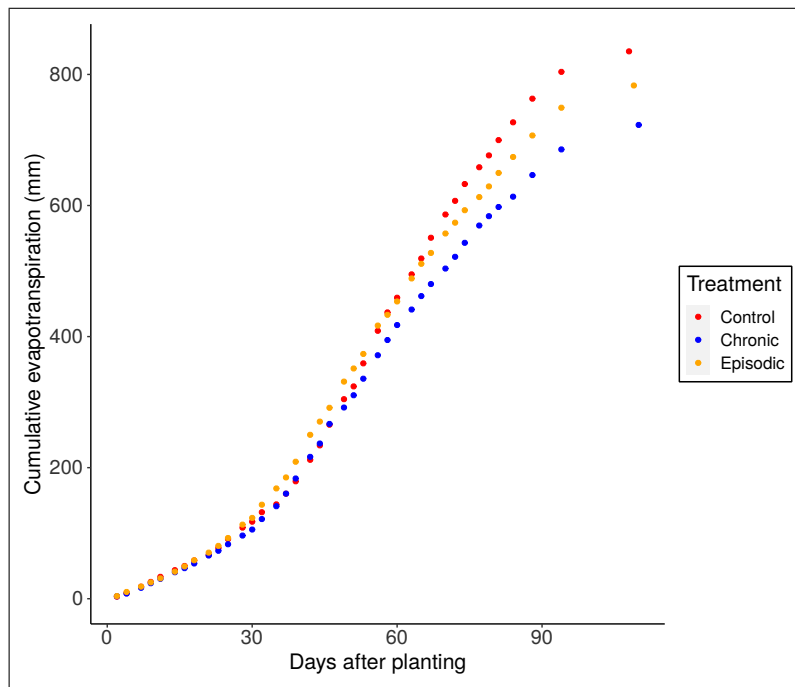


Figure 2: Cumulative evapotranspiration (CET) (mm) of wheat variety Lennox from planting to harvest for Control, Chronic and Episodic O<sub>3</sub> treatment.

CET exhibited a significant response to O<sub>3</sub> in both the Episodic and Chronic treatment, which showed 6.2% and 13.4% lower end-of-season CET respectively in comparison with the Control (Fig. 2). Nevertheless, the O<sub>3</sub> impact varied in magnitude with time and the plant sensitivity to O<sub>3</sub> was investigated according to the growth stage. The crop cycle was separated into three stages, from seed germination (ZS 01) to the first node stage (ZS 31) (Stage 1), the first node stage to the end of anthesis (ZS 69) (Stage 2) and from the end of anthesis to harvest maturity (ZS 99) (Stage 3). We used the Pearson test to examine the differences in CET between the Control and Chronic as well as Control and Episodic treatment (Table 2). During Stage 1,

there was a weak, non-significant correlation between the two variables (p-value >0.05). At that stage, only the plants in the Chronic treatment were fumigated with O<sub>3</sub>. This shows that the effect of O<sub>3</sub> before ZS 31 was not significant. On the other hand, during Stages 2 and 3 there was a significant positive correlation in the difference in CET between Control and Chronic and Control and Episodic treatment (i.e. p-value < 0.001 in both stages). This implies that the O<sub>3</sub> impact was significant during Stages 2 and 3. Thus, the negative effects of O<sub>3</sub> on wheat were considered to initiate at the onset of stem elongation (ZS 31) until crop maturity.

	corr	p-value	Test
Stage 1	0.28	0.28	Pearson
Stage 2	0.98	<0.001	Pearson
Stage 3	0.97	<0.001	Pearson

Table 2: Correlation coefficients for difference in cumulative evapotranspiration (CET) between Control and Chronic as well as Control and Episodic O<sub>3</sub> treatment. Stage 1 is from seed germination (ZS 01) to first node (ZS 31), Stage 2 is from first node to end of anthesis (ZS 69) and Stage 3 is from end of anthesis to harvest maturity (ZS 99).

Next, we calculated the percentage change in CET (pCET) between the control and O<sub>3</sub>-fumigated plants as follows:

$$pCET_{oz} = (CET_{cc} - CET_{oz})/CET_{oz} \quad (5)$$

$$pCET_{ep.oz} = (CET_{cc} - CET_{ep.oz})/CET_{ep.oz} \quad (6)$$

where pCET<sub>oz</sub> is the percentage change in CET between the Control and Chronic treatment and pCET<sub>ep.oz</sub> is the percentage change in CET between the Control and Episodic treatment. Since only the differences after Stage 1 were considered, we normalized pCET<sub>oz</sub> and pCET<sub>ep.oz</sub> by subtracting their value at the end of Stage 1. We also calculated the AOT40 index for the same time period (i.e. for Stages 2 and 3).

Fig. 3 (a) shows that the plants in the Episodic treatment were significantly more affected by the O<sub>3</sub> exposure than the plants in the Chronic treatment and exhibited higher values of pCET. In other words, the plants which started in the low O<sub>3</sub> environment and were transferred to high O<sub>3</sub> at ZS 31 were more sensitive to the pollutant than the plants which grew at high [O<sub>3</sub>] from emergence. Thus, the early fumigation with O<sub>3</sub> in the Chronic treatment decreased the plant sensitivity later in the season. This is in accordance with previous studies which report that the priming of plants can lead to improved performance at a subsequent abiotic stress event (Tanou et al., 2012; Wang et al., 2014; Li et al., 2014). The plants in the Episodic treatment were not fumigated with O<sub>3</sub> at Stage 1 and exhibited higher sensitivity to the pollutant during Stage 2.

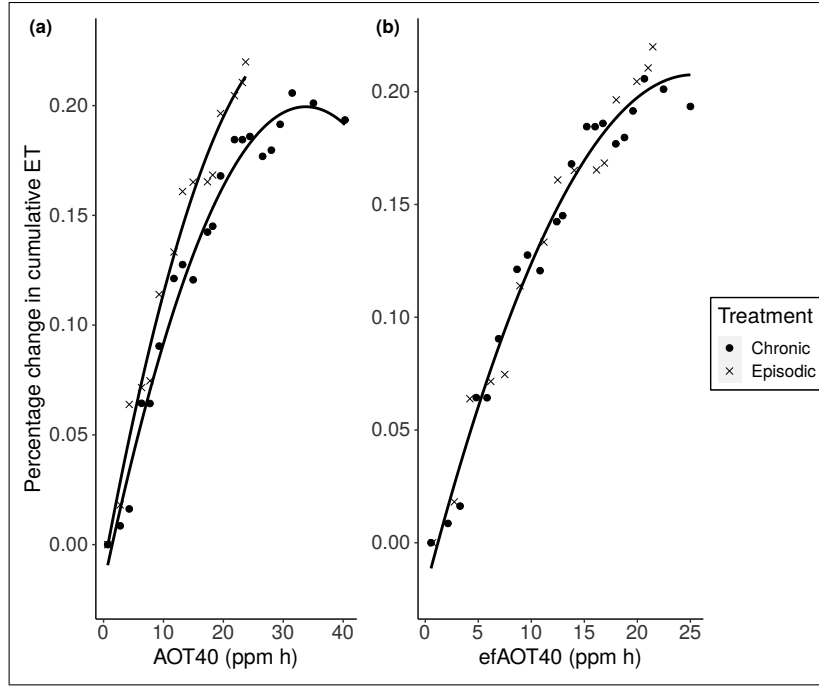


Figure 3: (a) Percentage change in cumulative evapotranspiration (pCET) of wheat variety Lennox between Control and Chronic treatment as well as Control and Episodic  $O_3$  treatment plotted against AOT40; (b) pCET expressed as function of effective AOT40 (efAOT40) and continuous black line is the regression:  $y = -0.021 + 0.018x - 0.000356x^2$  ( $R^2=0.98$ ,  $p < 0.01$ ). All pCET values were calculated for Stages 2, 3 after normalization at the end of Stage 1. AOT40 and efAOT40 were calculated for the same stages.

### 2.6.2. Acclimation factor

The duration of plant exposure to  $O_3$  affected the relationship between pCET and AOT40 (Fig. 3 (a)). We introduced the effective AOT40 index (efAOT40) which accounts for the variability in the effect of  $O_3$  on wheat over time. The efAOT40 index represents the part of daily  $O_3$  exposure which is limiting for the plant growth and is defined as:

$$efAOT40 = \sum_{i=1}^n (1 - f_{acl_i}) DOE40_i \quad (7)$$

where  $n$  is the number of days in the growing season,  $i$  is the day index and  $f_{acl}$  is an acclimation factor that accounts for the plant adjustment to  $O_3$  over time.  $f_{acl}$  is a function of the number of days that DOE40 is above zero ( $ND_{oz}$ ), it is in the  $[0,1]$  range and is updated in daily time step as follows:

$$f_{acl} = a_1 * f(ND_{oz}) \quad (8)$$

where  $a_1$  is an empirical constant and  $ND_{oz}$  starts at zero at planting and is updated in daily time step as follows:

$$ND_{oz(i)} = \begin{cases} ND_{oz(i-1)} + 1 & DOE40_i > 0 \\ ND_{oz(i-1)} & DOE40_i = 0 \end{cases} \quad (9)$$

where  $i$  is the day after planting and  $i-1$  is the previous day.

Due to incomplete understanding of the plant acclimation process to chronic  $O_3$  stress, different equations were tested for the parameterization of  $f_{acl}$ . We evaluated the fit of a linear, quadratic and square root function in the expression of  $f_{acl}$  against  $ND_{oz}$  (Table 3). The parameter  $a_1$  was calibrated to minimize RMSE for pCET between the Chronic and Episodic treatment when expressed against efAOT40. RMSE was calculated as follows:

$$RMSE = \sqrt{\frac{\sum_{i=1}^n (pCET_{oz_i} - pCET_{ep.oz_i})^2}{n}} \quad (10)$$

where  $i$  is the day index and  $n$  is the number of observations.

For the derivation of Eq. 8, the linear shape was selected since it provided the lowest RMSE between all functions tested (Table 3). The relationship between pCET and efAOT40 was described by a second degree polynomial model (Fig. 3 (b)), which was used in GLAM-ROC to estimate the  $O_3$ -induced reduction on potential ET (i.e. the canopy ET rate under optimal growth conditions). Detailed information about the incorporation of the above-mentioned formula into the model is given in the Appendix A.3.

Line shape	Function	Calibrated value of $a_1$	RMSE
Linear	$a_1 ND_{oz}$	0.006	0.0124
Quadratic	$a_1 ND_{oz}^2$	0.0001	0.0182
Root	$a_1 \sqrt{ND_{oz}}$	0.05	0.0136

Table 3: Evaluation of different line shapes in the expression of acclimation factor ( $f_{acl}$ ) as function of the number of days of  $O_3$  exposure ( $ND_{oz}$ ). The empirical parameter  $a_1$  was calibrated to minimize RMSE between  $pCET_{oz}$  and  $pCET_{ep.oz}$  when expressed against efAOT40.

### 2.6.3. Ozone effects on transpiration efficiency and partitioning to grains

Exposure to  $O_3$  induces up-regulation of the plant antioxidant metabolism which is energy demanding and the plants suppress their growth to use their resources for reducing the stress damage (Betzberger et al., 2010; Fatima et al., 2019). As a result TE decreases, since the plant growth reduction exceeds the reduction in ET (VanLoocke et al., 2012). HI also decreases due to reduced allocation of assimilates to the grains (Pleijel et al., 2014).

In GLAM-ROC, we applied  $O_3$ -induced modifications on both TE and the rate of increase of HI (dHI/dt). TE is defined as:

$$TE = \min\left(\frac{E_T}{VPD}, E_{TN,max}\right) \quad (11)$$

where  $E_T$  is normalised transpiration efficiency in Pa, VPD is vapour pressure deficit (kPa), and  $E_{TN,max}$  is

the maximum transpiration efficiency in  $\text{g kg}^{-1}$ . In this study, temperature and humidity were controlled (see Table 1) and VPD did not fluctuate significantly for most of the days in the growing season, thus for simplicity TE was set equal to  $E_{\text{TN,max}}$ . The effect of  $\text{O}_3$  on TE was related to the effective  $[\text{O}_3]$  index ( $ef[\text{O}_3]$ ). This index is calculated similarly to  $ef\text{AOT40}$  to simulate the plant adjustment to chronic  $\text{O}_3$  stress which leads to optimization of biomass productivity over time.  $ef[\text{O}_3]$  is a fraction of daily  $[\text{O}_3]$  defined as follows:

$$ef[\text{O}_3] = (1 - f_{acl}) \cdot [\text{O}_3] \quad (12)$$

where  $[\text{O}_3]$  is the daily mean  $\text{O}_3$  concentration during the daylight hours and  $f_{acl}$  is calculated in Eq. 8. For  $d\text{HI}/dt$ , no acclimation mechanism was assumed to impact on the allocation of assimilates to the grains, thus the effect was related to  $[\text{O}_3]$ .

The effects of  $\text{O}_3$  on both TE and  $d\text{HI}/dt$  were initiated above 10 ppb which is the  $\text{O}_3$  level of the pre-industrial period (Marenco et al., 1994). This threshold was set since GLAM-ROC is designed to simulate the effect of  $\text{O}_3$  pollution on wheat in comparison with the pre-industrial period. TE and  $d\text{HI}/dt$  decreased linearly above the 10 ppb  $[\text{O}_3]$  threshold as follows (Fig. 4):  $ef[\text{O}_3]$  is a fraction of daily  $[\text{O}_3]$  defined as follows:

$$\frac{TE_{oz}}{TE_c} = \begin{cases} 1 & [\text{O}_3] < 10\text{ppb} \\ c_1 \cdot ef[\text{O}_3] + d_1 & [\text{O}_3] \geq 10\text{ppb} \end{cases} \quad (13)$$

$$\frac{(d\text{HI}/dt)_{oz}}{(d\text{HI}/dt)_c} = \begin{cases} 1 & ef[\text{O}_3] < 10\text{ppb} \\ c_2 \cdot ef[\text{O}_3] + d_2 & ef[\text{O}_3] \geq 10\text{ppb} \end{cases} \quad (14)$$

where  $TE_c$ ,  $TE_{oz}$ ,  $(d\text{HI}/dt)_c$  and  $(d\text{HI}/dt)_{oz}$  are the control and  $\text{O}_3$ -limited TE and  $d\text{HI}/dt$  respectively.

Feng et al. (2008) summarizes various experiments with wheat plants fumigated with different  $\text{O}_3$  levels. The study finds that the aboveground biomass is decreased by an average of 18% at  $[\text{O}_3]$  of 72 ppb in comparison with carbon-filtered treatments. Similarly, HI reduces by 9% at the same  $[\text{O}_3]$  level. Following the above findings, the slope and intercept of Eq. 13, 14 were calculated accordingly and their values are given in Table A.5.

## 2.7. Model calibration and evaluation measures

The GLAM-ROC model was calibrated against the observed data for KWS Bittern wheat in the Control treatment. The metric used for the model calibration was the absolute error (AE) according to the following formula:

$$AE = |O - S| \quad (15)$$

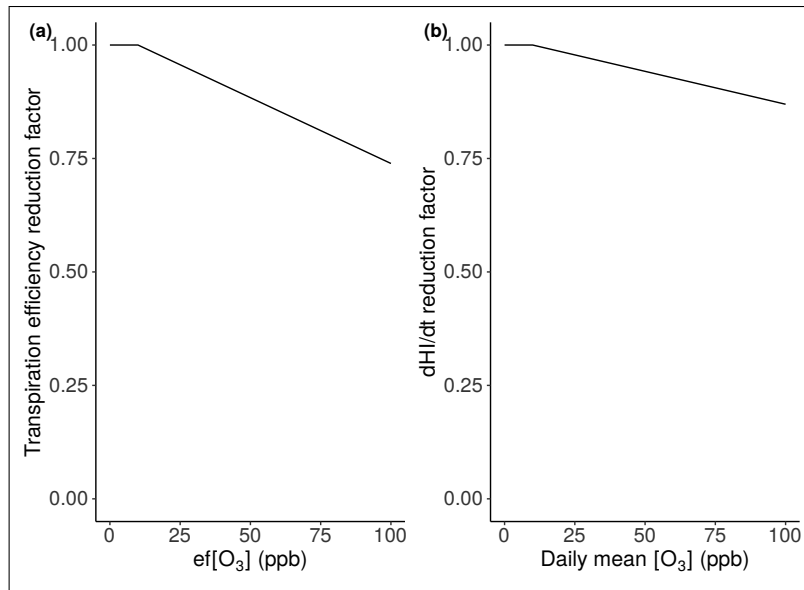


Figure 4: O<sub>3</sub>-induced reduction (a) in transpiration efficiency (TE) relative to control expressed against effective daily mean [O<sub>3</sub>] (ef[O<sub>3</sub>]), (b) in the rate of increase of HI (dHI/dt) relative to control expressed as function of daily mean [O<sub>3</sub>].

where O and S are the observed and simulated values of the compared variables. The model performance was evaluated with the absolute percent error between the observed and simulated value of all compared variables.

## 2.8. Calibration

The phenology of the model was set to meet the observed anthesis and maturity dates of the Control treatment. This was done to avoid any model bias from sources different than the O<sub>3</sub> stress effects. The maximum transpiration efficiency ( $E_{TN,max}$ ) was calibrated with the use of an optimizer which selected the value that minimized AE between the end-of-season observed and simulated above-ground biomass in the Control treatment. Similarly, the rate of change of harvest index (dHI/dt) was selected by the optimizer to minimize AE between the observed and simulated grain yield of the Control treatment. The step for the runs of the optimizer was 0.1 for  $E_{TN,max}$  and 0.0005 for dHI/dt. The ranges and values of the calibrated parameters are provided in Table A.6. All other parameter values were taken from Droutsas et al. (2019). The yield gap parameter (YGP) was set to one since O<sub>3</sub> was the only yield-limiting factor.

## 2.9. Sensitivity analysis

We performed a sensitivity analysis to test GLAM-ROC in a wide range of O<sub>3</sub> concentrations. The relative O<sub>3</sub> damage to yield was examined in comparison with the yield at the baseline O<sub>3</sub> concentration. In the meta-analysis of Pleijel et al. (2018), average [O<sub>3</sub>] of charcoal-filtered air treatments was 13.3 ppb. We used the

same baseline for direct comparison between the two studies. We modified all hourly O<sub>3</sub> concentrations in the Chronic and Episodic treatment by the appropriate value, such that the average [O<sub>3</sub>] during the growing season was [13.3, 23.3, ..., 83.3 ppb]. We run GLAM-ROC at the different O<sub>3</sub> concentration levels by keeping all other environmental conditions constant. The relative O<sub>3</sub> damages to yield in the Chronic and Episodic treatment were calculated as percentage differences in yield from the baseline simulation.

### 3. Results

#### 3.1. Evaluation of GLAM-ROC model skill

Exposure to O<sub>3</sub> significantly decreased the plant biomass and yield of KWS Bittern wheat in the experiments as well as the total evapotranspiration (TET) and WUE. All measured and simulated values of the compared variables and their percent error are shown in Table 4. The model reproduced the observed plant biomass response in both O<sub>3</sub> treatments (Fig. 5(a)). In the Chronic treatment, the percent error between the observed and simulated biomass at harvest was 5.02%. In the Episodic treatment, biomass was simulated to within 1% of observation. Thus, the model closely followed the effect of O<sub>3</sub> stress on wheat biomass in both durations of exposure by accounting for O<sub>3</sub>-induced reductions in canopy ET and TE.

	Control			Chronic			Episodic		
	Measured	Simulated	Percent error (%)	Measured	Simulated	Percent error (%)	Measured	Simulated	Percent error (%)
Biomass	2643.1	2659.0	0.60	2075.1	1971.0	5.02	2169.5	2185.0	0.71
Yield	1114.8	1113.0	0.16	738.2	738.0	0.03	913.0	915.0	0.22
HI	0.422	0.419	0.71	0.356	0.374	5.06	0.420	0.419	0.24
TET difference									
from control (%)	-	-	-	-12.10	-14.54	20.17	-9.42	-10.14	7.64
WUE difference									
from control (%)	-	-	-	-9.98	-13.27	32.97	-9.27	-8.55	7.77

Table 4: Measured and simulated above-ground biomass (g m<sup>-2</sup>), grain yield (g m<sup>-2</sup>), harvest index (HI), total ET (TET) and WUE difference from control (%) as well as their percent error in Control, Chronic and Episodic O<sub>3</sub> treatment.

Regarding the grain yield, GLAM-ROC accurately estimated the observed decreases in both the Chronic and Episodic treatment. Yield was simulated to within 1% of observation in both the Chronic and Episodic treatment. Reduction in HI was also noticed in the Chronic but not the Episodic treatment (Fig. 6). This was due to lack of O<sub>3</sub> fumigation during the grain filling period in the Episodic treatment. The model reproduced the observed plant response to HI in the Episodic treatment where the simulated value was within 1% of observation. In the Chronic treatment, HI was overestimated by 5.06%.

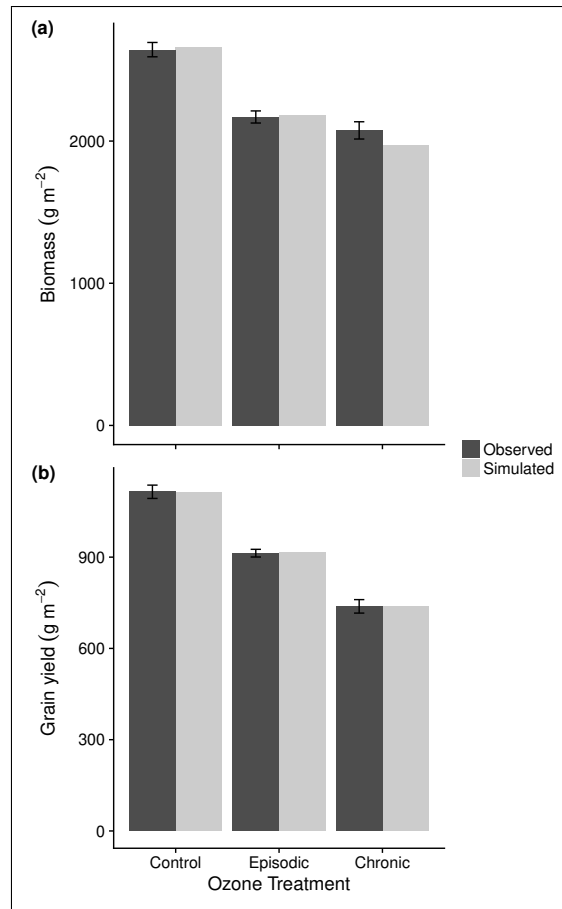


Figure 5: Observed (wheat variety KWS Bittern) and simulated (a) above-ground biomass and (b) grain yield at harvest in Control, Chronic and Episodic O<sub>3</sub> treatment. Error bars are standard errors of means in the observations.

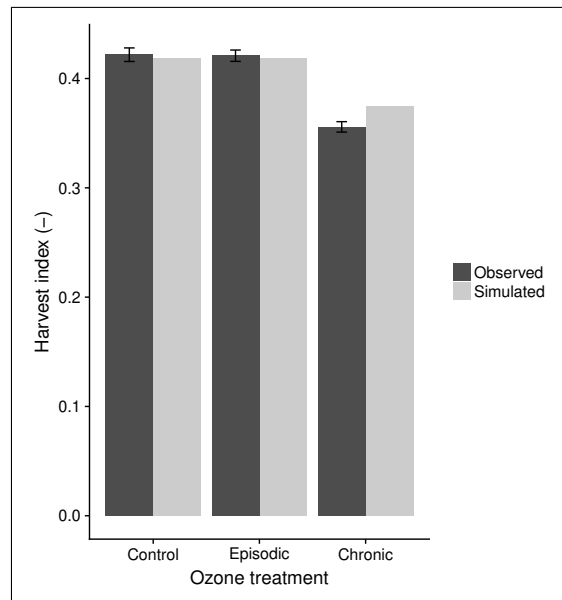


Figure 6: Observed (wheat variety KWS Bittern) and simulated harvest index in Control, Chronic and Episodic O<sub>3</sub> treatment. Error bars are standard errors of means in the observations.

Finally, GLAM-ROC overestimated the O<sub>3</sub>-induced reduction in TET in the Chronic treatment and the percent error was 20.17% (Fig. 7 (a)). The model skill was higher in the Episodic treatment where the percent error was 7.64%. WUE was significantly overestimated in the Chronic treatment, where the percent error was 32.97 % (Fig. 7 (b)). In the Episodic treatment, GLAM-ROC exhibited improved skill and the percent error for WUE was 7.77%.

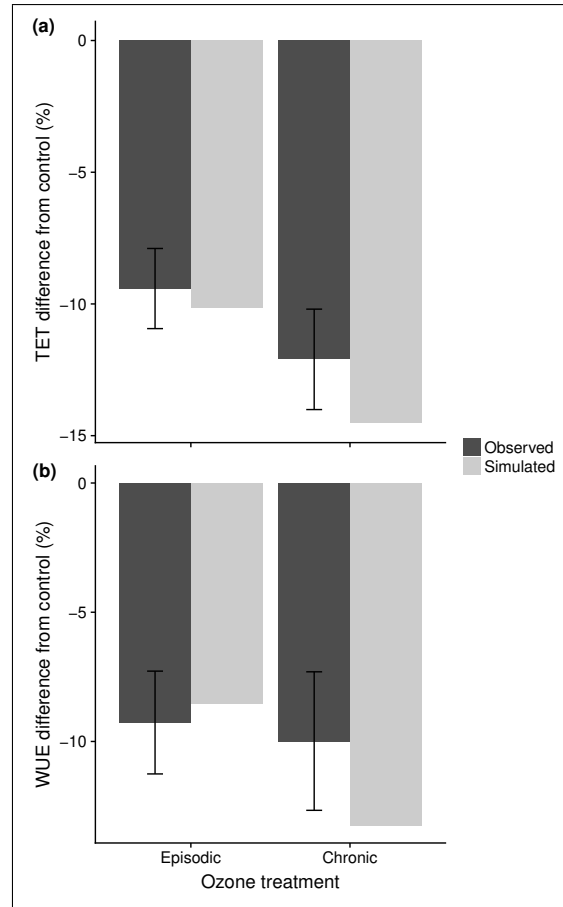


Figure 7: Observed (wheat variety KWS Bittern) and simulated difference from control in end-of season (a) total evapotranspiration (TET) and (b) water use efficiency (WUE) in Chronic and Episodic O<sub>3</sub> treatment. Error bars are standard errors of means in the observations.

### 3.2. Sensitivity of GLAM-ROC to different O<sub>3</sub> concentrations

Yield reduction was higher in the Chronic than the Episodic exposure in all O<sub>3</sub> concentrations (Fig. 8). In the Episodic treatment, yield reduced in an almost linear fashion for every 10 ppb increase in [O<sub>3</sub>] from the baseline. Using linear regression of the data points, yield loss was found to increase by 0.28% per ppb increase in [O<sub>3</sub>] (regression not shown). In the Chronic treatment, yield loss increased by 0.54% per ppb increase in [O<sub>3</sub>] (regression not shown), however the standard error (se) of the slope was 177.3% higher than the Episodic treatment (i.e. se of slope was 0.0366 in Chronic against 0.0132 in Episodic treatment). This means that in the Chronic treatment, the reduction in grain yield diverted substantially from the linear line

depending on  $[O_3]$ . The highest yield loss was estimated when the difference from the baseline  $[O_3]$  value increased from 30 to 40 ppb. In absolute numbers, the grain yield of wheat was most affected when  $[O_3]$  increased from 43.3 to 53.3 ppb. Within that concentration range, the average damage to yield was 0.96% per ppb increase in  $[O_3]$ . In the Episodic treatment, the same  $[O_3]$  range gave the highest damage to yield with 0.39% loss per ppb increase in  $[O_3]$ .

We also applied linear regression to all data points in the Chronic and Episodic treatment and compared the regression line to those developed in the meta-analysis of Pleijel et al. (2018) and Broberg et al. (2015) (Fig. 8). The three lines were in close agreement with each other and the slope of this study was -0.41 against -0.36 of Pleijel et al. (2018) and -0.47 of Broberg et al. (2015). Thus, the studies suggest 0.41%, 0.36% and 0.47% increase in wheat yield loss respectively per ppb increase in  $[O_3]$  above the baseline. However, it should be noted that the lower  $O_3$  damage suggested by Pleijel et al. (2018) in comparison to Broberg et al. (2015) may be explained by that the former study used wheat yield data only from charcoal-filtered and non-filtered air treatments, whilst the latter study used also treatments with elevated  $O_3$  levels. In addition, the meta-analysis of Feng et al. (2008) estimates that the grain yield of wheat is reduced by 17.5 and 29% at average  $[O_3]$  of 43 and 72 ppb respectively. Both findings are in very close agreement with the regression line of our study which predicted the loss in grain yield with less than 3% difference from the reported values (Fig. 8). Overall, GLAM-ROC was in accordance with the existing meta-analysis studies and closely followed the measured effect of  $O_3$  on the grain yield of wheat.

### *3.3. GLAM-ROC comparison with ozone exposure response function*

A large number of studies estimate the regional or global effect of  $O_3$  on crop productivity based on a statistical response function (SRF) between the relative crop yield and the level of  $O_3$  exposure (e.g. Hollaway et al., 2012; Ghude et al., 2014; Sharma et al., 2019). This formula assumes linear reduction in grain yield in relation to AOT40. The modelling methodology introduced in GLAM-ROC assumes non-linear  $O_3$  effect on yield with increased exposure to the pollutant. The two methods were evaluated against the observed data for KWS Bittern wheat. In the SRF model, the function for wheat was taken from Mills et al. (2007). The AOT40 index was accumulated during Stages 2 and 3, since these days were the most  $O_3$ -sensitive (i.e. the last 68 days of the crop season).

In GLAM-ROC, the grain yield in the Chronic treatment was 80.7% of the Episodic, which was less than 1% different from the observed value (Fig. 9). In the SRF model, the Chronic: Episodic yield ratio was 0.35, underestimated by 56.5%. This was due to the overestimation of the  $O_3$  damage to yield at a greater extent in

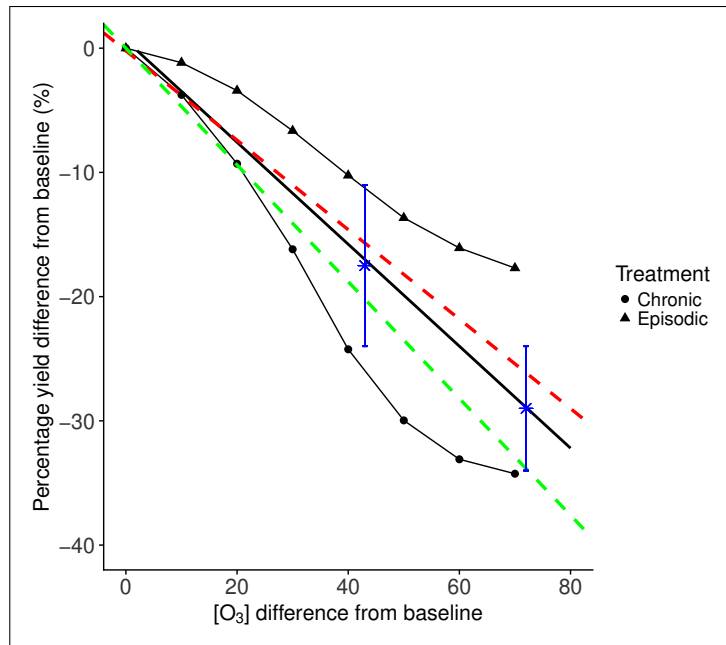


Figure 8: GLAM-ROC estimations of  $O_3$ -induced grain yield loss of wheat at different  $O_3$  concentrations in Chronic (circles) and Episodic treatment (triangles) in comparison with baseline. Solid black line is linear regression of all data points in Chronic and Episodic treatment, red and green dashed lines are linear regressions in meta-analysis of Pleijel et al. (2018) and Broberg et al. (2015) respectively. Star data points are  $O_3$ -induced yield losses at 43 and 72 ppb  $[O_3]$  in meta-analysis of Feng et al. (2008) and error bars are 95% confidence intervals. The two star data points are presented using their absolute  $[O_3]$  value on x axis instead of the difference from baseline, since this was not reported.

the Chronic than the Episodic treatment. Nevertheless, no acclimation mechanism is considered in the SRF model and the  $O_3$  damage to yield is linearly extrapolated as AOT40 increases. As a result, the observed non-linear plant response with increased exposure to  $O_3$  stress affected the skill of the model. Thus, GLAM-ROC improved upon the SRF model in the estimation of the Chronic: Episodic yield ratio by accounting for the plant acclimation to chronic  $O_3$  stress at variable duration of exposure.

#### 4. Discussion

We developed and evaluated the GLAM-ROC model to simulate the effect of  $O_3$  on wheat growth and development. The model successfully reproduced the  $O_3$ -induced damage to wheat biomass and yield in both the Episodic and Chronic treatment. The plant biomass was simulated to within 6% of observation in both durations of exposure. Similarly, the simulated grain yield was less than 1% different from the measurements. The model also closely followed the observed effects of  $O_3$  on HI, ET and WUE.

The modelling approach followed here is simpler than stomatal flux-based methods commonly used in crop models. Such method was avoided since it strongly depends on stomatal conductance, a trait which is highly

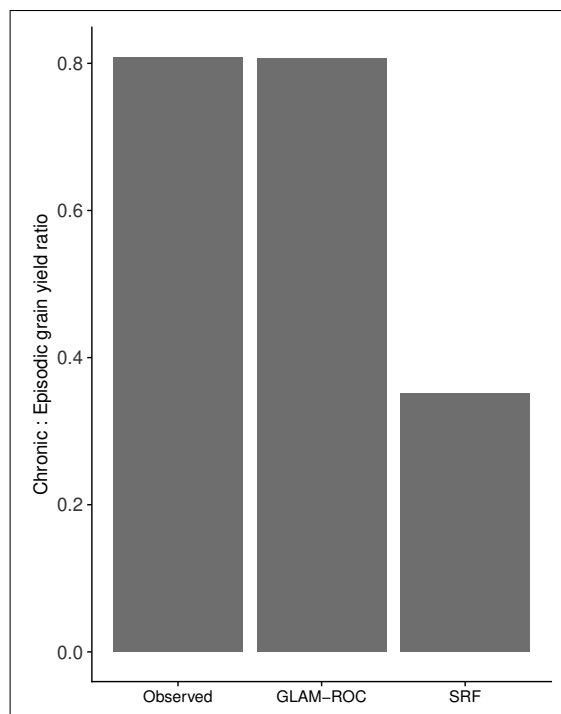


Figure 9: Observed and simulated grain yield in Chronic relative to Episodic treatment. SRF is statistical response function for wheat taken from Mills et al. (2007).

complex (Buckley, 2017) and not simple to incorporate in process-based crop models. Difficulties may also be faced in crop models with complex  $O_3$  schemes regarding their parameterization for large scale applications (Emberson et al., 2018). GLAM is a large area crop model and unwarranted complexity should be avoided (Challinor et al., 2018). In addition, our approach – even relying on an exposure-based methodology – overcomes some limitations of the statistical response function. This is due to relating AOT40 to the potential ET rate instead of using the index to estimate grain yield loss directly. ET and AOT40 have been previously seen to correlate significantly under well-watered conditions (Jaudé et al., 2008; VanLoocke et al., 2012). Nevertheless, the use of AOT40 disregards the effect of  $O_3$  stress on ET below 40 ppb. Bernacchi et al. (2011) and VanLoocke et al. (2012) exposed soybean plants to various  $O_3$  concentrations and showed that the pollutant reduces canopy ET significantly for exposures above 40 ppb. Since wheat and soybean exhibit similar sensitivity to  $O_3$  (Mills et al., 2007), in our study we also related the reduction in canopy ET to the AOT40 index.

In GLAM-ROC, the  $O_3$ -induced decrease in ET is estimated in comparison with the same plant growing in optimal environment. Under water stress, the effect of  $O_3$  on crop growth can be reduced due to decreased stomatal conductance and lower uptake of the pollutant by the leaves (Khan and Soja, 2003; Feng et al., 2008). Both  $O_3$  and drought reduce the daily canopy transpiration rate in the model, the minimum of which

is considered as the actual transpiration (i.e. the effect of drought (Challinor et al., 2004) and O<sub>3</sub> (this study) on ET are estimated independently). Thus, if limited soil water suppresses transpiration to a greater extent than O<sub>3</sub>, there will be no additive effect of the pollutant on canopy ET. In other words, the O<sub>3</sub> damage to crop transpiration and growth decreases with higher levels of water stress in GLAM-ROC. The accuracy of this approach should be tested against experimental data with wheat exposed to both stressors simultaneously. In this study, GLAM-ROC was only evaluated for the effect of O<sub>3</sub> on well-watered wheat crops. Thus, the model can be currently used only in regions where adequate rainfall prevents water stress or where wheat is fully irrigated. Elevated CO<sub>2</sub> concentrations can also reduce stomatal conductance and protect against O<sub>3</sub> pollution (Yadav et al., 2019). Currently, GLAM-ROC does not account for the effect of elevated CO<sub>2</sub> on crop growth and yield, thus it cannot be used for future environments with rising CO<sub>2</sub> concentrations (i.e. the model has to be calibrated each time for the given CO<sub>2</sub> level). Following the addition of the CO<sub>2</sub> fertilization mechanism, the interaction between elevated CO<sub>2</sub> and O<sub>3</sub> should be addressed to allow for the estimation of crop performance and yield under future climate change conditions.

GLAM-ROC uses the acclimation factor to simulate the plant adaptation to chronic O<sub>3</sub> stress. This was necessary for capturing the differences in water consumption and biomass productivity between the Chronic and Episodic treatment. The plants in the Chronic treatment exhibited higher values of water consumption than the Episodic during their common period of O<sub>3</sub> fumigation (i.e. at Stage 2). Nevertheless, only the plants in Chronic treatment were exposed to high O<sub>3</sub> during Stage 1. The lack of previous exposure to the stressor in the Episodic treatment increased the plant sensitivity at Stage 2, thus reducing the water consumption rates. This difference in plant behaviour could not be simulated without considering the effect of plant acclimation to chronic O<sub>3</sub> exposure. The acclimation factor was calculated according to the number of days of O<sub>3</sub> fumigation, thus modifying the plant sensitivity to O<sub>3</sub> at different durations of exposure. The same factor simulated the differences in biomass productivity between the two O<sub>3</sub> exposures through modifying the effect on TE. The SRF model does not account for the plant acclimation mechanism and overestimated the relative damage to grain yield between the Chronic and Episodic treatment by 56.5%.

In GLAM-ROC, the acclimation factor was related to the 40 ppb threshold (Eq. 8, 9), which means that no plant acclimation was considered for exposure to O<sub>3</sub> below that level. This threshold was chosen since it is the most commonly used threshold for relating the O<sub>3</sub> exposure to loss in crop yield (e.g., Fuhrer et al., 1997; Mills et al., 2011; Sharma et al., 2019). However, it is unclear if this is the optimal threshold for wheat acclimation to the pollutant or if it needs to be adjusted in the future. In our study, the O<sub>3</sub> concentrations in

the chambers were either very low (below 10 ppb in the Control treatment) or significantly higher than 40 ppb during exposure to the pollutant in the Chronic and Episodic treatments. Thus, decreasing the acclimation threshold does not change the model results in comparison with the observations (Section 3.1). In addition, the sensitivity analysis (Section 3.2) indicates that this threshold is appropriate, since the model can be reliably used for simulating grain yield losses for O<sub>3</sub> exposure below 40 ppb. Nevertheless, since wheat performance is affected by O<sub>3</sub> below 40 ppb (Pleijel, 2011), the plant acclimation threshold may need to be reconsidered in the future.

The plant sensitivity to O<sub>3</sub> varies also according to the growth stage. O<sub>3</sub> did not exhibit significant effect on wheat from plant emergence to ZS 31, at least in terms of water consumption. Thus, the O<sub>3</sub> damage to wheat was simulated to initiate at ZS 31. On the other hand, the period from anthesis to the end of grain filling is the most O<sub>3</sub>-sensitive for grain yield reduction (Lee et al., 1988; Pleijel et al., 1998; Soja et al., 2000). The Episodic treatment was not fumigated with high O<sub>3</sub> after anthesis and HI was less than 1% different from the Control. In the Chronic treatment, HI was 14.3% lower than the Control due to high O<sub>3</sub> exposure during grain filling. GLAM-ROC was able to reproduce the O<sub>3</sub>-induced reduction to yield by slowing down the daily rate of increase of HI (dHI/dt) based on the [O<sub>3</sub>] level. As a result, the model followed the observed decrease in HI and successfully simulated the O<sub>3</sub> impact on grain yield at maturity.

The development and evaluation of GLAM-ROC were based on controlled-environment chamber experiments where the environmental conditions cannot perfectly match the field. For instance, the plants were grown in pots instead of being rooted on the ground. Nevertheless, the meta-analysis of Feng and Kobayashi (2009) revealed no significant differences in the yield response to O<sub>3</sub> between pot and ground-rooted wheat plants. In addition, the daily O<sub>3</sub> concentration in the chambers did not match the diurnal variation experienced under ambient conditions (e.g. Pawlak and Jarosławski, 2015; Wang et al., 2017). However, Harmens et al. (2018) exposed a modern wheat variety to various background O<sub>3</sub> concentrations and different peak O<sub>3</sub> episodes and showed that the relationship between the reduction in grain yield and the accumulated stomatal O<sub>3</sub> flux could be explained by the same slope irrespective of the temporal O<sub>3</sub> profile. Moreover, in our study the fumigation in the Chronic treatment lasted for the full crop cycle (i.e. 107 days) with an average concentration of 78.8 ppb, which can be unrealistic for most parts of the world. The highest frequency of O<sub>3</sub> pollution episodes (i.e. daily average 8-h [O<sub>3</sub>] of at least 75 ppb) in the summertime for the year 2000 was 38 days in North America (Lei et al., 2012). The Episodic treatment was closer to these conditions with the total duration of plant O<sub>3</sub> exposure being 33 days. The real dynamics of surface O<sub>3</sub> in polluted regions are likely

to be between the Episodic and Chronic treatments of this study. In addition, the average CO<sub>2</sub> concentration in the chambers was around 530 ppm and this concentration level was experienced in all treatments. For this reason, CO<sub>2</sub> was not accounted as an additional varying factor in the estimation of O<sub>3</sub> damage to wheat.

Our sensitivity analysis suggested 0.41% average yield loss per ppb increase in O<sub>3</sub> concentration above 13.3 ppb, which is directly comparable with existing meta-analysis studies (Fig. 8). In the Chronic treatment, the model estimated a 0.96% maximum damage to yield per ppb increase in O<sub>3</sub> concentration, which occurred when [O<sub>3</sub>] was in the 43.3 - 53.3 ppb range. In the Episodic treatment, the same concentration range gave the maximum damage to yield per ppb increase in [O<sub>3</sub>], which was considerably lower at 0.39%. Overall, the yield loss per ppb increase in [O<sub>3</sub>] varied from 0.17% to 0.96%, depending on the treatment (i.e. Chronic vs. Episodic) and the [O<sub>3</sub>] level. Hence, the duration of exposure to O<sub>3</sub> stress is a significant factor influencing the effect of the pollutant on wheat productivity and yield. Longer duration of exposure to O<sub>3</sub> implies higher reduction in yield, however the relative damage may decrease as the duration increases. The non-linear grain yield vs. [O<sub>3</sub>] pattern can result from enhanced plant acclimation with increased duration exposure to the pollutant. Thus, we believe that the plant acclimation process should be taken into account for robust estimation of the chronic effect of O<sub>3</sub> on crop growth, productivity and yield.

## 5. Conclusion

Exposure to O<sub>3</sub> significantly decreased the wheat biomass and grain yield in the experiments. The GLAM-ROC crop model was developed and evaluated for the effect of O<sub>3</sub> on wheat growth and development. A statistical relationship was introduced to estimate the reduction in canopy evapotranspiration based on the O<sub>3</sub> exposure (i.e. AOT40 index). Decreases in transpiration efficiency and harvest index were also incorporated into the model according to the O<sub>3</sub> concentration. The model successfully reproduced the observed O<sub>3</sub> damage to biomass and yield of KWS Bittern wheat in both the Episodic and Chronic treatment. Accounting for the plant acclimation to chronic O<sub>3</sub> stress was necessary for good model skill. The acclimation process was empirically incorporated with the use of an acclimation factor based on the days of O<sub>3</sub> exposure. This allowed the simulation of plant adjustment to O<sub>3</sub> over time which reduced the relative damage to biomass and yield. The statistical response function ignored the acclimation process and overestimated the Chronic: Episodic grain yield ratio. It is concluded that the plant acclimation to chronic O<sub>3</sub> stress is significant and should be taken into account for the estimation of the O<sub>3</sub> damage to wheat growth and productivity.

## Acknowledgements

This work was supported by the UK N8 AgriFood Resilience Programme. I.D. gratefully acknowledges the 'Oatley PhD Scholarship' and the Priestley International Centre for Climate for the financial support. The experimental data is generated as a part of the Joint Programming Initiative on Agriculture, Food Security and Climate Change (FACCE-JPI) and funded by the FACCE-ERA-NET+project: Climate-CAFÉ. We also thank the two anonymous reviewers whose comments have significantly improved this manuscript.

## References

- Ainsworth, E. A., 2017. Understanding and improving global crop response to ozone pollution. *The Plant Journal* 90 (5), 886–897.
- Arnold, S., Lombardozzi, D., Lamarque, J.-F., Richardson, T., Emmons, L., Tilmes, S., Sitch, S., Folberth, G., Hollaway, M., Val Martin, M., 2018. Simulated global climate response to tropospheric ozone-induced changes in plant transpiration. *Geophysical Research Letters* 45 (23), 13–070.
- Ashmore, M., 2005. Assessing the future global impacts of ozone on vegetation. *Plant, Cell & Environment* 28 (8), 949–964.
- Avnery, S., Mauzerall, D. L., Liu, J., Horowitz, L. W., 2011. Global crop yield reductions due to surface ozone exposure: 1. year 2000 crop production losses and economic damage. *Atmospheric Environment* 45 (13), 2284–2296.
- Barnes, J., Velissariou, D., Davison, A., Holevas, C., 1990. Comparative ozone sensitivity of old and modern greek cultivars of spring wheat. *New Phytologist* 116 (4), 707–714.
- Bernacchi, C. J., Leakey, A. D., Kimball, B. A., Ort, D. R., 2011. Growth of soybean at future tropospheric ozone concentrations decreases canopy evapotranspiration and soil water depletion. *Environmental pollution* 159 (6), 1464–1472.
- Betzberger, A. M., Gillespie, K. M., Mcgrath, J. M., Koester, R. P., Nelson, R. L., Ainsworth, E. A., 2010. Effects of chronic elevated ozone concentration on antioxidant capacity, photosynthesis and seed yield of 10 soybean cultivars. *Plant, Cell & Environment* 33 (9), 1569–1581.
- Borrell, A. K., Incoll, L., Simpson, R. J., Dalling, M. J., 1989. Partitioning of dry matter and the deposition and use of stem reserves in a semi-dwarf wheat crop. *Annals of Botany* 63 (5), 527–539.

- Broberg, M. C., Feng, Z., Xin, Y., Pleijel, H., 2015. Ozone effects on wheat grain quality—a summary. *Environmental pollution* 197, 203–213.
- Bruce, T. J., Matthes, M. C., Napier, J. A., Pickett, J. A., 2007. Stressful “memories” of plants: evidence and possible mechanisms. *Plant Science* 173 (6), 603–608.
- Buckley, T. N., 2017. Modeling stomatal conductance. *Plant physiology*, pp–01772.
- Buckley, T. N., Mott, K. A., 2013. Modelling stomatal conductance in response to environmental factors. *Plant, cell & environment* 36 (9), 1691–1699.
- Burney, J., Ramanathan, V., 2014. Recent climate and air pollution impacts on indian agriculture. *Proceedings of the National Academy of Sciences* 111 (46), 16319–16324.
- Challinor, A., Wheeler, T., Craufurd, P., Slingo, J., Grimes, D., 2004. Design and optimisation of a large-area process-based model for annual crops. *Agricultural and forest meteorology* 124 (1-2), 99–120.
- Challinor, A. J., Ewert, F., Arnold, S., Simelton, E., Fraser, E., 2009. Crops and climate change: progress, trends, and challenges in simulating impacts and informing adaptation. *Journal of experimental botany* 60 (10), 2775–2789.
- Challinor, A. J., Müller, C., Asseng, S., Deva, C., Nicklin, K. J., Wallach, D., Vanuytrecht, E., Whitfield, S., Ramirez-Villegas, J., Koehler, A.-K., 2018. Improving the use of crop models for risk assessment and climate change adaptation. *Agricultural systems* 159, 296–306.
- Chen, C. P., Frei, M., Wissuwa, M., 2011. The *ozt8* locus in rice protects leaf carbon assimilation rate and photosynthetic capacity under ozone stress. *Plant, cell & environment* 34 (7), 1141–1149.
- Christy, B., Tausz-Posch, S., Tausz, M., Richards, R., Rebetzke, G., Condon, A., McLean, T., Fitzgerald, G., Bourgault, M., O'leary, G., 2018. Benefits of increasing transpiration efficiency in wheat under elevated  $CO_2$  for rainfed regions. *Global change biology* 24 (5), 1965–1977.
- Damour, G., Simonneau, T., Cochard, H., Urban, L., 2010. An overview of models of stomatal conductance at the leaf level. *Plant, Cell & Environment* 33 (9), 1419–1438.
- Droutsas, I., Challinor, A., Swiderski, M., Semenov, M. A., 2019. New modelling technique for improving crop model performance-application to the glam model. *Environmental Modelling & Software* 118, 187–200.

- Emberson, L., Ashmore, M., Cambridge, H., Simpson, D., Tuovinen, J.-P., 2000. Modelling stomatal ozone flux across Europe. *Environmental Pollution* 109 (3), 403–413.
- Emberson, L., Büker, P., Ashmore, M., Mills, G., Jackson, L., Agrawal, M., Atikuzzaman, M., Cinderby, S., Engardt, M., Jamir, C., et al., 2009. A comparison of north American and Asian exposure–response data for ozone effects on crop yields. *Atmospheric Environment* 43 (12), 1945–1953.
- Emberson, L. D., Pleijel, H., Ainsworth, E. A., Van den Berg, M., Ren, W., Osborne, S., Mills, G., Pandey, D., Dentener, F., Büker, P., et al., 2018. Ozone effects on crops and consideration in crop models. *European Journal of Agronomy* 100, 19–34.
- Ewert, F., Porter, J. R., 2000. Ozone effects on wheat in relation to CO<sub>2</sub>: modelling short-term and long-term responses of leaf photosynthesis and leaf duration. *Global Change Biology* 6 (7), 735–750.
- FAO, I., UNICEF, et al., 2017. WFP, WHO (2017) the state of food security and nutrition in the world 2017. Building Resilience for Peace and Food Security (Food and Agriculture Organization, Rome).
- Farage, P., Long, S. P., 1999. The effects of O<sub>3</sub> fumigation during leaf development on photosynthesis of wheat and pea: an in vivo analysis. *Photosynthesis Research* 59 (1), 1–7.
- Farage, P. K., Long, S. P., Lechner, E. G., Baker, N. R., 1991. The sequence of change within the photosynthetic apparatus of wheat following short-term exposure to ozone. *Plant Physiology* 95 (2), 529–535.
- Fatima, A., Singh, A. A., Mukherjee, A., Agrawal, M., Agrawal, S. B., 2019. Ascorbic acid and thiols as potential biomarkers of ozone tolerance in tropical wheat cultivars. *Ecotoxicology and Environmental Safety* 171, 701–708.
- Feng, Z., Kobayashi, K., 2009. Assessing the impacts of current and future concentrations of surface ozone on crop yield with meta-analysis. *Atmospheric Environment* 43 (8), 1510–1519.
- Feng, Z., Kobayashi, K., Ainsworth, E. A., 2008. Impact of elevated ozone concentration on growth, physiology, and yield of wheat (*Triticum aestivum* L.): a meta-analysis. *Global Change Biology* 14 (11), 2696–2708.
- Feng, Z., Wang, L., Pleijel, H., Zhu, J., Kobayashi, K., 2016. Differential effects of ozone on photosynthesis of winter wheat among cultivars depend on antioxidative enzymes rather than stomatal conductance. *Science of the Total Environment* 572, 404–411.

- Fiscus, E. L., Booker, F. L., Burkey, K. O., 2005. Crop responses to ozone: uptake, modes of action, carbon assimilation and partitioning. *Plant, Cell & Environment* 28 (8), 997–1011.
- Frenck, G., van der Linden, L., Mikkelsen, T. N., Brix, H., Jørgensen, R. B., 2011. Increased [co<sub>2</sub>] does not compensate for negative effects on yield caused by higher temperature and [o<sub>3</sub>] in *brassica napus* L. *European Journal of Agronomy* 35 (3), 127–134.
- Fuhrer, J., Skärby, L., Ashmore, M. R., 1997. Critical levels for ozone effects on vegetation in Europe. *Environmental Pollution* 97 (1-2), 91–106.
- Ghude, S. D., Jena, C., Chate, D., Beig, G., Pfister, G., Kumar, R., Ramanathan, V., 2014. Reductions in India's crop yield due to ozone. *Geophysical Research Letters* 41 (15), 5685–5691.
- Gillespie, K. M., Rogers, A., Ainsworth, E. A., 2011. Growth at elevated ozone or elevated carbon dioxide concentration alters antioxidant capacity and response to acute oxidative stress in soybean (*Glycine max*). *Journal of Experimental Botany* 62 (8), 2667–2678.
- Gillespie, K. M., Xu, F., Richter, K. T., McGrath, J. M., Markelz, R. C., Ort, D. R., Leakey, A. D., Ainsworth, E. A., 2012. Greater antioxidant and respiratory metabolism in field-grown soybean exposed to elevated O<sub>3</sub> under both ambient and elevated CO<sub>2</sub>. *Plant, Cell & Environment* 35 (1), 169–184.
- Hansen, E. M., Hauggaard-Nielsen, H., Launay, M., Rose, P., Mikkelsen, T. N., 2019. The impact of ozone exposure, temperature and CO<sub>2</sub> on the growth and yield of three spring wheat varieties. *Environmental and Experimental Botany*, 103868.
- Harmens, H., Hayes, F., Mills, G., Sharps, K., Osborne, S., Pleijel, H., 2018. Wheat yield responses to stomatal uptake of ozone: Peak vs rising background ozone conditions. *Atmospheric Environment* 173, 1–5.
- Heath, R. L., 1994. Possible mechanisms for the inhibition of photosynthesis by ozone. *Photosynthesis Research* 39 (3), 439–451.
- Heath, R. L., Lefohn, A. S., Musselman, R. C., 2009. Temporal processes that contribute to nonlinearity in vegetation responses to ozone exposure and dose. *Atmospheric Environment* 43 (18), 2919–2928.
- Held, A., Mooney, H., Gorham, J. N., 1991. Acclimation to ozone stress in radish: leaf demography and photosynthesis. *New Phytologist* 118 (3), 417–423.

- Hollaway, M. J., Arnold, S., Challinor, A. J., Emberson, L., 2012. Intercontinental trans-boundary contributions to ozone-induced crop yield losses in the northern hemisphere. *Biogeosciences* 9 (1), 271–292.
- Ingvordsen, C. H., Backes, G., Lyngkjær, M. F., Peltonen-Sainio, P., Jensen, J. D., Jalli, M., Jahoor, A., Rasmussen, M., Mikkelsen, T. N., Stockmarr, A., et al., 2015. Significant decrease in yield under future climate conditions: Stability and production of 138 spring barley accessions. *European Journal of Agronomy* 63, 105–113.
- Jaudé, M. B., Katerji, N., Mastrorilli, M., Rana, G., 2008. Analysis of the effect of ozone on soybean in the mediterranean region: I. the consequences on crop-water status. *European Journal of Agronomy* 28 (4), 508–518.
- Khan, S., Soja, G., 2003. Yield responses of wheat to ozone exposure as modified by drought-induced differences in ozone uptake. *Water, Air, and Soil Pollution* 147 (1-4), 299–315.
- Kollist, H., Zandalinas, S. I., Sengupta, S., Nuhkat, M., Kangasjärvi, J., Mittler, R., 2018. Rapid responses to abiotic stress: priming the landscape for the signal transduction network. *Trends in plant science*.
- Lee, E. H., Tingey, D. T., Hogsett, W. E., 1988. Evaluation of ozone exposure indices in exposure-response modeling. *Environmental Pollution* 53 (1-4), 43–62.
- Lei, H., Wuebbles, D. J., Liang, X.-Z., 2012. Projected risk of high ozone episodes in 2050. *Atmospheric environment* 59, 567–577.
- Li, X., Cai, J., Liu, F., Dai, T., Cao, W., Jiang, D., 2014. Cold priming drives the sub-cellular antioxidant systems to protect photosynthetic electron transport against subsequent low temperature stress in winter wheat. *Plant Physiology and Biochemistry* 82, 34–43.
- Lombardozzi, D., Levis, S., Bonan, G., Sparks, J., 2012. Predicting photosynthesis and transpiration responses to ozone: decoupling modeled photosynthesis and stomatal conductance. *Biogeosciences Discussions* 9 (4).
- Marenco, A., Gouget, H., Nédélec, P., Pagés, J.-P., Karcher, F., 1994. Evidence of a long-term increase in tropospheric ozone from pic du midi data series: Consequences: Positive radiative forcing. *Journal of Geophysical Research: Atmospheres* 99 (D8), 16617–16632.

- Mauzerall, D. L., Wang, X., 2001. Protecting agricultural crops from the effects of tropospheric ozone exposure: reconciling science and standard setting in the united states, europe, and asia. *Annual Review of energy and the environment* 26 (1), 237–268.
- McGrath, J. M., Betzelberger, A. M., Wang, S., Shook, E., Zhu, X.-G., Long, S. P., Ainsworth, E. A., 2015. An analysis of ozone damage to historical maize and soybean yields in the united states. *Proceedings of the National Academy of Sciences* 112 (46), 14390–14395.
- Mikkelsen, T. N., Ro-Poulsen, H., 1994. Exposure of norway spruce to ozone increases the sensitivity of current year needles to photoinhibition and desiccation. *New Phytologist* 128 (1), 153–163.
- Mills, G., Buse, A., Gimeno, B., Bermejo, V., Holland, M., Emberson, L., Pleijel, H., 2007. A synthesis of aot40-based response functions and critical levels of ozone for agricultural and horticultural crops. *Atmospheric Environment* 41 (12), 2630–2643.
- Mills, G., Hayes, F., Simpson, D., Emberson, L., Norris, D., Harmens, H., Büker, P., 2011. Evidence of widespread effects of ozone on crops and (semi-) natural vegetation in europe (1990–2006) in relation to aot40-and flux-based risk maps. *Global Change Biology* 17 (1), 592–613.
- Mills, G., Sharps, K., Simpson, D., Pleijel, H., Frei, M., Burkey, K., Emberson, L., Uddling, J., Broberg, M., Feng, Z., et al., 2018. Closing the global ozone yield gap: Quantification and cobenefits for multistress tolerance. *Global change biology* 24 (10), 4869–4893.
- Moot, D., Jamieson, P., Henderson, A., Ford, M., Porter, J., 1996. Rate of change in harvest index during grain-filling of wheat. *The Journal of Agricultural Science* 126 (4), 387–395.
- Mulholland, B., Craigan, J., Black, C., Colls, J., Atherton, J., Landon, G., 1998. Effects of elevated co2 and o3 on the rate and duration of grain growth and harvest index in spring wheat (*triticum aestivum* L.). *Global Change Biology* 4 (6), 627–635.
- Musselman, R. C., Lefohn, A. S., Massman, W. J., Heath, R. L., 2006. A critical review and analysis of the use of exposure-and flux-based ozone indices for predicting vegetation effects. *Atmospheric Environment* 40 (10), 1869–1888.
- Pawlak, I., Jarosławski, J., 2015. The influence of selected meteorological parameters on the concentration of surface ozone in the central region of poland. *Atmosphere-Ocean* 53 (1), 126–139.

- Pleijel, H., 2011. Reduced ozone by air filtration consistently improved grain yield in wheat. *Environmental pollution* 159 (4), 897–902.
- Pleijel, H., Broberg, M. C., Uddling, J., Mills, G., 2018. Current surface ozone concentrations significantly decrease wheat growth, yield and quality. *Science of the Total Environment* 613, 687–692.
- Pleijel, H., Danielsson, H., Emberson, L., Ashmore, M., Mills, G., 2007. Ozone risk assessment for agricultural crops in europe: Further development of stomatal flux and flux–response relationships for european wheat and potato. *Atmospheric Environment* 41 (14), 3022–3040.
- Pleijel, H., Danielsson, H., Gelang, J., Sild, E., Selldén, G., 1998. Growth stage dependence of the grain yield response to ozone in spring wheat (*triticum aestivum* L.). *Agriculture, ecosystems & environment* 70 (1), 61–68.
- Pleijel, H., Danielsson, H., Ojanperä, K., De Temmerman, L., Högy, P., Badiani, M., Karlsson, P., 2004. Relationships between ozone exposure and yield loss in european wheat and potato—a comparison of concentration- and flux-based exposure indices. *Atmospheric Environment* 38 (15), 2259–2269.
- Pleijel, H., Danielsson, H., Simpson, D., Mills, G., 2014. Have ozone effects on carbon sequestration been overestimated? a new biomass response function for wheat. *Biogeosciences* 11 (16), 4521–4528.
- Ratjen, A., Lemaire, G., Kage, H., Plénet, D., Justes, E., 2018. Key variables for simulating leaf area and n status: Biomass based relations versus phenology driven approaches. *European Journal of Agronomy* 100, 110–117.
- Reyenga, P. J., Howden, S. M., Meinke, H., McKeon, G. M., 1999. Modelling global change impacts on wheat cropping in south-east queensland, australia. *Environmental modelling & software* 14 (4), 297–306.
- Schauberger, B., Rolinski, S., Schaphoff, S., Müller, C., 2019. Global historical soybean and wheat yield loss estimates from ozone pollution considering water and temperature as modifying effects. *Agricultural and Forest Meteorology* 265, 1–15.
- Sharma, A., Ojha, N., Pozzer, A., Beig, G., Gunthe, S. S., 2019. Revisiting the crop yield loss in india attributable to ozone. *Atmospheric Environment: X* 1, 100008.
- Sicard, P., Anav, A., Marco, A. D., Paoletti, E., 2017. Projected global ground-level ozone impacts on vegetation under different emission and climate scenarios. *Atmospheric Chemistry and Physics* 17 (19), 12177–12196.

- Siddique, K., Kirby, E., Perry, M., 1989. Ear: stem ratio in old and modern wheat varieties; relationship with improvement in number of grains per ear and yield. *Field Crops Research* 21 (1), 59–78.
- Soja, G., Barnes, J., Posch, M., Vandermeiren, K., Pleijel, H., Mills, G., 2000. Phenological weighting of ozone exposures in the calculation of critical levels for wheat, bean and plantain. *Environmental Pollution* 109 (3), 517–524.
- Tanou, G., Fotopoulos, V., Molassiotis, A., 2012. Priming against environmental challenges and proteomics in plants: update and agricultural perspectives. *Frontiers in Plant Science* 3, 216.
- Temple, P., 1986. Stomatal conductance and transpirational responses of field-grown cotton to ozone. *Plant, Cell & Environment* 9 (4), 315–321.
- Tiedemann, A., Pfähler, B., 1994. Growth stage-dependent effects of ozone on the permeability for ions and non-electrolytes of wheat leaves in relation to the susceptibility to septoria nodorum berk. *Physiological and molecular plant pathology* 45 (2), 153–167.
- Van Goethem, T., Azevedo, L., Van Zelm, R., Hayes, F., Ashmore, M., Huijbregts, M., 2013. Plant species sensitivity distributions for ozone exposure. *Environmental pollution* 178, 1–6.
- VanLoocke, A., Betzelberger, A. M., Ainsworth, E. A., Bernacchi, C. J., 2012. Rising ozone concentrations decrease soybean evapotranspiration and water use efficiency whilst increasing canopy temperature. *New Phytologist* 195 (1), 164–171.
- Wang, W.-N., Cheng, T.-H., Gu, X.-F., Chen, H., Guo, H., Wang, Y., Bao, F.-W., Shi, S.-Y., Xu, B.-R., Zuo, X., et al., 2017. Assessing spatial and temporal patterns of observed ground-level ozone in china. *Scientific reports* 7 (1), 3651.
- Wang, X., Vignjevic, M., Jiang, D., Jacobsen, S., Wollenweber, B., 2014. Improved tolerance to drought stress after anthesis due to priming before anthesis in wheat (*triticum aestivum* L.) var. vinjett. *Journal of experimental botany* 65 (22), 6441–6456.
- Wilkinson, S., Mills, G., Illidge, R., Davies, W. J., 2012. How is ozone pollution reducing our food supply? *Journal of Experimental Botany* 63 (2), 527–536.
- Yadav, A., Bhatia, A., Yadav, S., Kumar, V., Singh, B., 2019. The effects of elevated co2 and elevated o3 exposure on plant growth, yield and quality of grains of two wheat cultivars grown in north india. *Heliyon* 5 (8), e02317.

## Appendix A.

### Appendix A.1. SLA function in GLAM-Parti

In Ratjen et al. (2018) the canopy SLA for wheat was expressed as function of LAI (Fig A.10). The suggested relationship is the following:

$$SLA = \begin{cases} 161.3 + 11.3 \cdot LAI & DVS < 32 \\ 137 + 15.1 \cdot LAI & DVS \geq 32 \end{cases} \quad (A.1)$$

For GLAM-Parti, the major limitation of the above piecewise function is the lack of continuity on the first day when DVS reaches 32 (i.e. Zadoks stage 32). In Fig. A.10, this day is shown in point (LAI1, SLA1). In order to deal with this discontinuity, the slope and intercept of Eq. A.1 were modified above DVS = 32 as:

$$SLA = \begin{cases} 161.3 + 11.3 \cdot LAI & DVS < 32 \\ z + y \cdot LAI & DVS \geq 32 \end{cases} \quad (A.2)$$

where y and z were determined using points (LAI1, SLA1) and (6, 227.6). The second point is the solution of Eq. A.1 for LAI = 6 and DVS ≥ 32. Based on the two points, y and z were calculated as:

$$y = (SLA1 - 227.6)/(LAI1 - 6) \quad (A.3)$$

$$z = 227.6 - 6 \cdot y \quad (A.4)$$

Eq. A.2 is used in GLAM-Parti to express SLA as function of LAI and graphical illustration is shown in Fig A.10 (b).

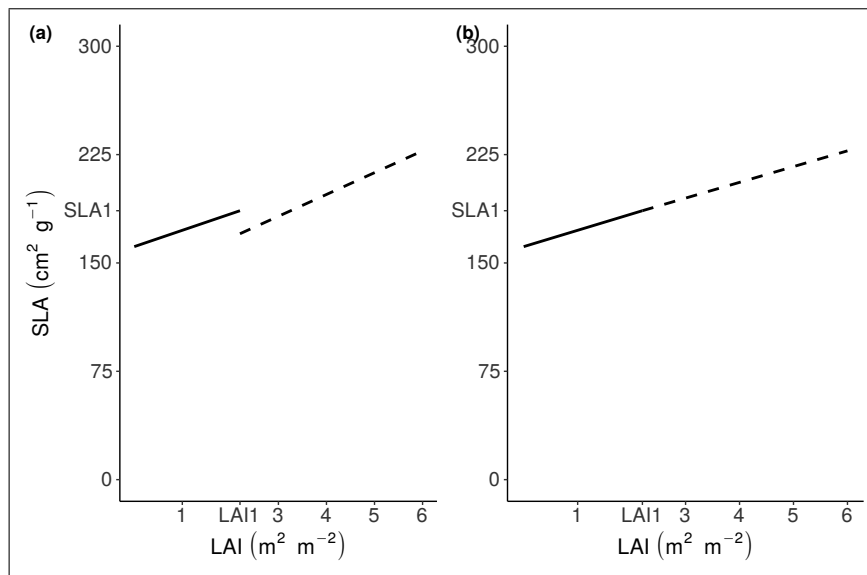


Figure A.10: Canopy SLA as function of LAI (a) in Ratjen et al. (2018) (b) in this study. Point (LAI1, SLA1) is when DVS reaches 32.

Appendix A.2. Expanding GLAM-Parti approach after anthesis

In GLAM-Parti, the above-ground biomass ( $W_n$ ) consists of leaves, stems, ears and grains as follows:

$$W_n = M_L + M_S + M_E + M_G \quad (\text{A.5})$$

where  $M_L$  is leaf,  $M_S$  is stem,  $M_E$  is the non-grain ear mass and  $M_G$  is the grain mass.  $M_E$  is expressed as function of  $M_S$  as follows:

$$M_E = C_E \cdot TT_n / TT_{fl} \cdot M_S \quad (\text{A.6})$$

where  $TT_n$  is the thermal time elapsed from terminal spikelet initiation (TS) until day  $n$  after TS and  $TT_{fl}$  is the thermal time requirement from TS to anthesis.  $C_E$  expresses the ratio of ear: stem mass at anthesis, which is set to 0.5 for modern wheat varieties (Siddique et al., 1989).  $M_G$  is expressed as function of  $W_n$  using the harvest index (HI) as follows:

$$M_G = HI \cdot W_n \quad (\text{A.7})$$

Eq. A.6, A.7 can be combined to describe Eq. A.5 as:

$$W_n = (1/(1 - HI)) \cdot (M_L + (1 + C_E \cdot TT_n / TT_{fl}) \cdot M_S) \quad (\text{A.8})$$

Eq. A.8 can be further manipulated to express  $W_n$  as function of leaf area change.  $M_L$  is expressed as:

$$M_L = LAI / SLA + M_{YL} \quad (\text{A.9})$$

where LAI is green leaf area index, SLA is canopy specific leaf area and  $M_{YL}$  is the mass of yellow leaves.

LAI can be expanded as:

$$LAI_n = LAI_{n-1} + dL \quad (\text{A.10})$$

where  $LAI_n$  is the value of LAI at any given  $n$  day,  $LAI_{n-1}$  is LAI of the previous day and  $dL$  is the leaf area change between the two consecutive days. The mass of stems ( $M_S$ ) is expressed with an allometric relationship according to  $M_L$  as:

$$M_S = h \cdot M_L^g \quad (\text{A.11})$$

where  $g$ ,  $h$  are allometric coefficients. Eq. A.2, A.9, A.10, A.11 can be combined to express Eq. A.8 as:

$$W_n = (1/(1 - HI)) \cdot \left( \frac{LAI_{n-1} + dL}{z + y \cdot (LAI_{n-1} + dL)} + M_{YL} + (1 + C_E \cdot TT_n / TT_{fl}) \cdot h \left( \frac{LAI_{n-1} + dL}{z + y \cdot (LAI_{n-1} + dL)} + M_{YL} \right)^g \right) \quad (\text{A.12})$$

where the slope and intercept of Eq. A.2 ( $y$ ,  $z$ ) vary before and after DVS = 32. Eq. A.12 expresses  $W_n$  as function of the leaf area change ( $dL$ ) and is used for the implementation of the SEMAC methodology during

the full crop cycle in GLAM-Parti. A detailed description of the SEMAC approach is given in Droutsas et al. (2019).

Moreover, the model was parameterized to account for the canopy leaf mass loss which mainly occurs during the period of rapid leaf senescence after anthesis. Whenever a negative value of leaf area change (dL) was estimated, the mass of yellow leaves ( $M_{YL}$ ) was updated as:

$$M_{YL(n)} = M_{YL(n-1)} + C_{yl} * (|dL|/SLA) \quad (\text{A.13})$$

where  $M_{YL(n)}$  is the mass of yellow leaves on the n day of the crop cycle,  $M_{YL(n-1)}$  is the mass of yellow leaves on the previous day (n-1), SLA is the canopy specific leaf area and  $C_{yl}$  is the ratio of yellow:green leaf mass which was set to 0.68 to account for the leaf mass loss due to the remobilization of dry mass (Borrell et al., 1989).

### Appendix A.3. $O_3$ effect on evapotranspiration in GLAM-ROC

The statistical formula for the expression of percentage change in cumulative evapotranspiration (pCET) according to effective AOT40 (efAOT40) is given below (Fig. 3 (b)):

$$pCET = -0.021 + 0.018 \cdot efAOT40 - 0.000356 \cdot efAOT40^2 \quad (\text{A.14})$$

where at any given n day of the growing season, pCET between the Control and  $O_3$  treatments is defined as:

$$pCET_n = \frac{CET_{AA_n} - CET_{oz_n}}{CET_{oz_n}} = \frac{CET_{AA_n}}{CET_{oz_n}} - 1 = \frac{CET_{AA_n}}{CET_{oz_{n-1}} + ET_{oz_n}} - 1 \quad (\text{A.15})$$

where  $CET_{AA}$  and  $CET_{oz}$  are the cumulative evapotranspiration of the control and  $O_3$  treatment respectively.

The substitution of Eq. A.15 into A.14 and solving for  $ET_{oz}$  gives:

$$ET_{oz_n} = \frac{CET_{AA_n}}{0.979 + 0.018 \cdot efAOT40 - 0.000365 \cdot efAOT40^2} - CET_{oz_{n-1}} \quad (\text{A.16})$$

Eq. A.16 is used in GLAM-ROC to calculate the  $O_3$ -induced decrease in ET ( $ET_{oz}$ ) in comparison with the same plant growing under optimal conditions.

TE reduction factor		dHI/dt reduction factor	
c1	d1	c2	d2
-0.0029	1.029	-0.00145	1.0145

Table A.5: Slope and intercept of O<sub>3</sub>-induced reduction in transpiration efficiency (TE) and rate of change in harvest index (dHI/dt) relative to Control.

Parameter	Unit	Range	GLAM-ROC value	Source
E <sub>TN,max</sub>	g kg <sup>-1</sup>	[3 - 10.6] <sup>a</sup>	9.3	Christy et al. (2018)
dHI/dt	day <sup>-1</sup>	[0.0064 - 0.0137]	0.0135	Moot et al. (1996)

Table A.6: Values and units of GLAM-ROC calibrated parameters.

<sup>a</sup> Average CO<sub>2</sub> concentration in the chambers was around 530 ppm (see Table 1). The upper boundary of E<sub>TN,max</sub> was multiplied by 1.18 to account for the CO<sub>2</sub> fertilization effect on TE (Reyenga et al., 1999).